Second-Order Self-Energy Calculations for Tightly Bound Electrons in Hydrogen-Like Ions

Igor A. Goidenko[1], Leonti N. Labzowsky[1], Andrei V. Nefiodov[2], Günter Plunien[3], Sven Zschocke[3], and Gerhard Soff[3]

[1] St. Petersburg State University, 198904 St. Petersburg, Russia
[2] Petersburg Nuclear Physics Institute, 188350 Gatchina, St. Petersburg, Russia
[3] Institut für Theoretische Physik, Technische Universität Dresden, Mommsenstrasse 13, 01062 Dresden, Germany

Abstract. The second-order electron self-energy is evaluated to all orders in the interaction with the Coulomb field of the nucleus for the ground state of hydrogen-like uranium ions. This completes the nonperturbative calculation of radiative corrections of order α^2. The major theoretical uncertainty is eliminated which provides predictions of the ground-state energy with a relative accuracy of about 10^{-6} for the uranium system. This allows for high-precision tests of QED in the strong field of the nucleus that are expected to be available experimentally in the near future.

1 Introduction

Heavy few-electron ions provide a unique testing ground for quantum electrodynamics (QED) in strong field of the nucleus. At SIS/ESR facilities in Darmstadt one is aiming at an accuracy of about 1eV in measurements of the ground-state Lamb shift for hydrogen-like uranium in the near future [1]. Theoretical evaluations on the same level of accuracy require calculations of the complete set of radiative corrections of the order α^2 but to all orders in the coupling constant $Z\alpha$ to the Coulomb field of nucleus. In this paper we report the recent status of this challenging theoretical problem for the most interesting cases of the hydrogen-like uranium and lead ions.

The complete set of second-order radiative corrections are displayed in Fig. 1. These diagrams are naturally divided into separately gauge invariant subsets: SESE a),b),c), VPVP d),e),f), SEVP g),h),i) and S(VP)E k). The abbreviation SE stands for self energy and VP denotes vacuum polarization. Most of these corrections have been already calculated numerically for $^{238}U^{91+}$ and $^{208}Pb^{81+}$ ions (see the latest reviews in [2,3]).

The VPVP contributions e) and f) (also known as Källén-Sabry corrections) have been investigated in Uehling approximation [4,5]. Calculating the dominat Uehling part of the lowest order VP correction leaves us with the accuracy of about 5% for the ground state of hydrogen-like U and Pb ions. Here one restricts to the first term in $Z\alpha$ expansion of the bound electron propagator in the electron

loop. This corresponds also to the expansion of the bound propagator in terms of the nuclear potential (see Fig. 2). Recently the VPVP e) contribution has been determined to all orders in $Z\alpha$ in [6]. In this case the inaccuracy of the Uehling approximation turned out to be about 25%. The exact VPVP d) contribution was tabulated in Refs. [7,8,4]. The SEVP g), h) and i) contributions were evaluated in Ref. [9] employing the Uehling approximation and in the exact form in Ref. [8]. The inaccuracy of Uehling approximation for hydrogen-like U reduces in this case to 2%. The S(VP)E contribution is known only in the Uehling approximation [9,10].

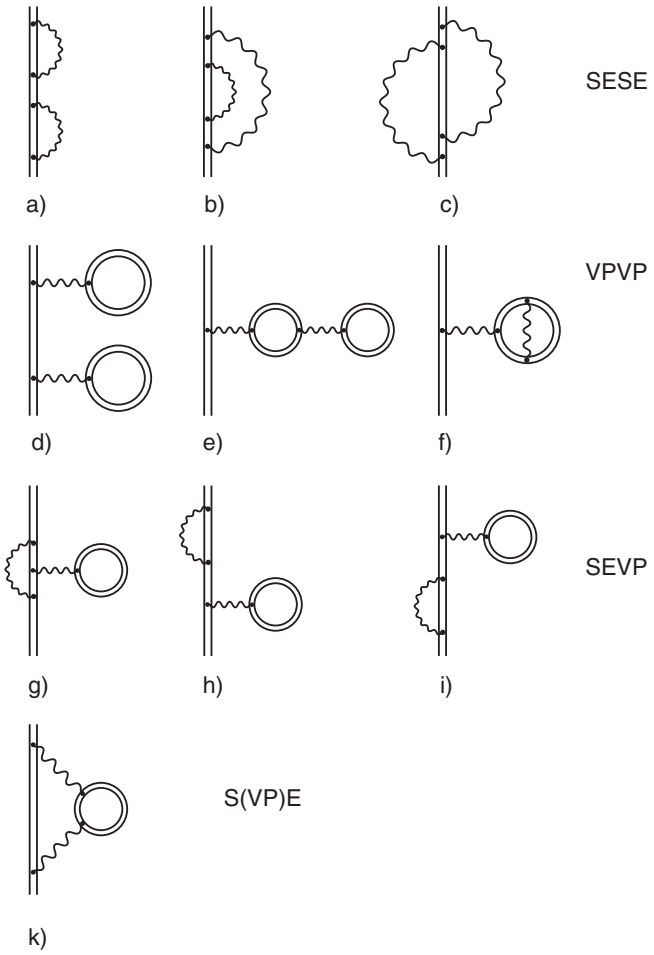

Fig. 1. Feynman diagrams corresponding to the second-order radiative corrections in H-like ions. The double solid line denotes the bound electron and the wavy line indicates the photon

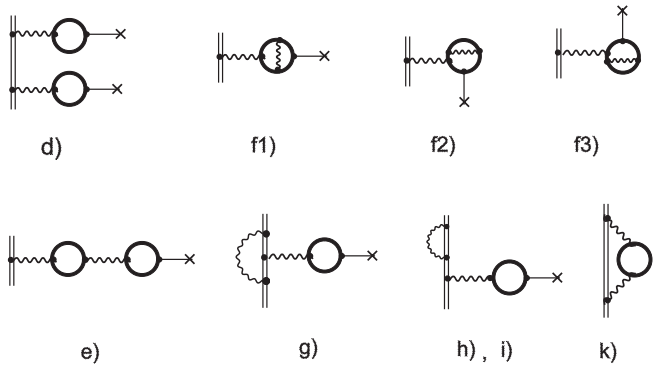

Fig. 2. Feynman graphs corresponding to VPVP and SEVP corrections in the Uehling approximation. The ordinary solid line denotes the free electron propagator. The line with the cross at the end denotes the nuclear potential. The other notations are the same as in Figure 1

2 Loop after loop irreducible SESE contribution

The diagram SESE a), that is called also "loop-after-loop", consists of irreducible and reducible parts (see Fig. 3). We consider first of all the irreducible contribution, which can be renormalized and evaluated separately since it does not contain infrared divergencies in the Feynman gauge. The renormalized expression for this contribution can be written as

$$\triangle E_a^{(\mathrm{irred})} = \sum_{n \neq a} \frac{\langle a|\gamma_0 \hat{\Sigma}^{(1)\mathrm{ren}}_{\mathrm{bou}}(E_a)|n\rangle\langle n|\gamma_0 \hat{\Sigma}^{(1)\mathrm{ren}}_{\mathrm{bou}}(E_a)|a\rangle}{E_a - E_n} \,, \tag{1}$$

where γ_0 is the Dirac matrix and $\hat{\Sigma}^{(1)\mathrm{ren}}_{\mathrm{bou}}$ is the renormalized lowest-order self energy operator for the bound electron. The notations $|n\rangle$, E_n refer to the Dirac atomic states and eigenvalues, the sum in Eq. (1) extends over the total Dirac spectrum for the electron in the field of the nucleus. The case $n = a$ corresponds to the reference state (later in this paper we will consider a as the ground state).

In Ref. [11] the corresponding energy shift has been calculated in the Feynman gauge for selected values of nuclear charge number $Z = 70, 80, 90$ and 92 and for the ground and few excited states for hydrogen-like ions. Here the covariant renormalization scheme based on the potential expansion was employed. This approach was first applied to bound electron calculations by Brown, Langer and Schaefer [12] and later developed and applied to the heavy hydrogen-like ions in [13]. The potential expansion for the lowest order SE is depicted in Fig. 4. With the use of this expansion one can cast the matrix elements in Eq. (1) into

$$\begin{aligned}\langle a|\gamma_0 \hat{\Sigma}^{(1)\mathrm{ren}}_{\mathrm{bou}}(E_a)|n\rangle = {} & \langle a|\gamma_0 \hat{\Sigma}^{ZP,\mathrm{ren}}_{\mathrm{bou}}(E_a)|n\rangle + \langle a|\gamma_0 \hat{\Sigma}^{OP,\mathrm{ren}}_{\mathrm{bou}}(E_a)|n\rangle \\ & + \langle a|\gamma_0 \hat{\Sigma}^{MP}_{\mathrm{bou}}(E_a)|n\rangle \,. \end{aligned} \tag{2}$$

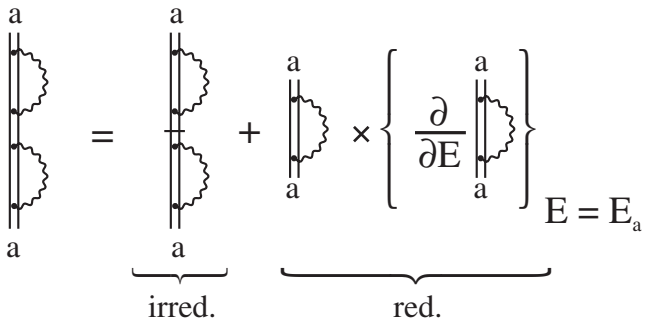

Fig. 3. The separation of the diagram SESE a) into irredcible and reducible parts. Here double solid line with the bar in the SESE a)-irred. part denotes the bound electron propagator with the excluded reference state a. The double solid line with the subscript E in the SESE a)-red. part denotes the bound electron propagator with the arbitrary energy parameter E

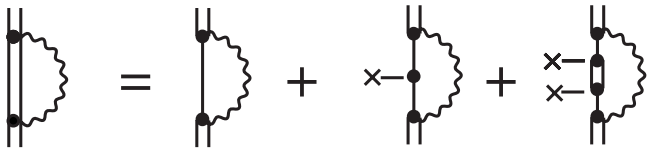

Fig. 4. The potential expansion of the lowest order self energy. Three terms of this expansion usually are denoted as zero-potential (ZP), one-potential (OP) and many-potential (MP). The notations are the same as in Figures 1, 2

Only the ZP and OP terms are divergent and therefore subject to renormalization. The MP term is finite, though most laborous in numerical evaluations. The renormalized expressions are

$$\hat{\Sigma}^{ZP,\mathrm{ren}}_{\mathrm{bou}} = \hat{\Sigma}^{(1)}(\not{p}) - \Sigma^{(1)} - \Sigma^{(1)'}(\not{p} - m)\,, \tag{3}$$

$$\hat{\Sigma}^{OP,\mathrm{ren}}_{\mathrm{bou}} = \hat{\Lambda}^{(1)}_{\mu} V_{\mu} - \gamma_{\mu} V_{\mu} \Lambda^{(1)}\,, \tag{4}$$

where $\hat{\Sigma}^{(1)}(\not{p})$ is the first-order SE operator for the free electron

$$\hat{\Sigma}^{(1)}(\not{p}) = -4\pi i\alpha \int \frac{d^4k}{(2\pi)^4} \gamma_{\mu} \frac{1}{\not{p} - \not{k} - m} \gamma^{\mu} \frac{1}{k^2} \tag{5}$$

and $\hat{\Lambda}^{(1)}_{\mu}$ is the lowest-order vertex function for the free electron

$$\hat{\Lambda}^{(1)}_{\mu}(\not{p}, \not{p}') = -4\pi i\alpha \int \frac{d^4k}{(2\pi)^4} \gamma_{\nu} \frac{1}{\not{p} - \not{k} - m} \gamma_{\mu} \frac{1}{\not{p} - \not{k} - m} \gamma^{\nu} \frac{1}{k^2}\,. \tag{6}$$

Here we introduced the standard mass counterterm

$$\delta m^{(1)} \equiv \Sigma^{(1)} \equiv \hat{\Sigma}^{(1)}(\not{p})\big|_{\not{p}=m}\,, \tag{7}$$

the charge counterterm

$$\gamma_\mu \Sigma^{(1')} = \left(\frac{\partial}{\partial p_\mu} \hat{\Sigma}^{(1)}(\not{p}) \right) |_{\not{p}=m} \tag{8}$$

and vertex counterterm

$$\gamma_\mu \Lambda^{(1)} \equiv \hat{\Lambda}^{(1)}_\mu(\not{p}, \not{p}')|_{\not{p}=\not{p}'=m} \, . \tag{9}$$

In Eqs. (5)–(9) V_μ stands for the external potential, the electric external potential corresponds to $V_0 \equiv V$, $\not{p} \equiv \gamma^\mu p_\mu$, m is the electron mass and α denotes the fine structure constant. We use the natural units $\hbar = c = 1$.

Eq. (2) presents the basis for the covariant renormalization approach. The explicit expressions are known for $\hat{\Sigma}^{ZP,\mathrm{ren}}_{\mathrm{bou}}(E)$, $\hat{\Sigma}^{OP,\mathrm{ren}}_{\mathrm{bou}}$ in momentum space. For obtaining these expressions the standard Feynman approach [11,12] or dimensional regularization [13] can be used. They are free from ultraviolet divergencies but acquire infrared divergencies after the renormalization. However, these infrared divergencies, contained in $\Sigma^{(1)'}$ and $\Lambda^{(1)}$, cancel due to the Ward identity $\Sigma^{(1)'} = -\Lambda^{(1)}$ and the use of the Dirac equation for the atomic electron in the reference state $|a\rangle$:

$$\gamma_0(\not{p} - m)|a\rangle = \hat{V}|a\rangle \, . \tag{10}$$

Using Eqs. (2)–(10) one can rewrite the matrix element for $\hat{\Sigma}^{\mathrm{ren}}_{\mathrm{bou}}$ also in the form:

$$\langle a|\gamma_0 \hat{\Sigma}^{(1)\mathrm{ren}}_{\mathrm{bou}}(E_a)|n\rangle = \langle a|\gamma_0 \hat{\Sigma}^{(1)}_{\mathrm{bou}}(E_a)|n\rangle - \delta m^{(1)} \langle a|\gamma_0|n\rangle \, , \tag{11}$$

where $\hat{\Sigma}^{(1)}_{\mathrm{bou}}$ is the unrenormalized expression for the first-order SE operator. Eq. (11) presents the basis for another popular renormalization approach, proposed in [14,15]. Within this approach Eq. (11) is replaced by the equation

$$\langle a|\gamma_0 \hat{\Sigma}^{(1)\mathrm{ren}}_{\mathrm{bou}}(E_a)|n\rangle = \langle a|\gamma_0 \hat{\Sigma}^{(1)}_{\mathrm{bou}}(E_a)|n\rangle - \langle a|\gamma_0 \hat{\Sigma}^{(1)}_{\mathrm{free}}|n\rangle \, . \tag{12}$$

In order to write down explicitely the matrix element $\langle |a\gamma_0 \hat{\Sigma}^{(1)}_{\mathrm{free}} n| \rangle$ the bound-state wave functions are expanded in terms of free-electron wave functions. The result is shown in Fig. 5. This renormalization approach can be called “direct”. The next step gave the name to the approach described: this is the partial wave expansion (PWE). Both terms on the right-hand side of Eq. (12) are expanded in partial waves. Then each term of this expansion both for $\hat{\Sigma}^{(1)}_{\mathrm{bou}}$ and $\hat{\Sigma}^{(1)}_{\mathrm{free}}$ is finite but the sum over partial waves is divergent. Combining both expansions one can write

$$\langle a|\gamma_0 \hat{\Sigma}^{(1)\mathrm{ren}}_{\mathrm{bou}}(E_a)|n\rangle = \sum_{l=0}^{\infty} \left(\langle a|\gamma_0 \hat{\Sigma}^{(1)l}_{\mathrm{bou}}(E_a)|n\rangle - \langle a|\gamma_0 \hat{\Sigma}^{(1)l}_{\mathrm{free}}|n\rangle \right) \, . \tag{13}$$

The sum over partial waves in Eq. (13) should be convergent in principle. The general explicit proof of this convergence is absent, but it can be justified in every particular case by observing the convergence in numerical calculations.

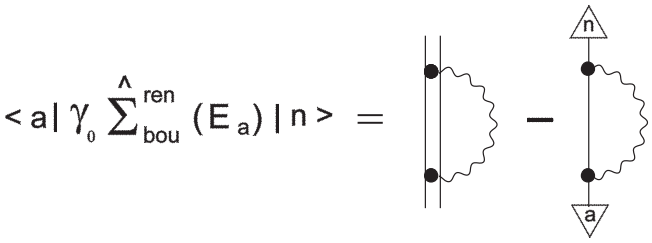

Fig. 5. The graphical representation of the "direct" renormalization approach. The triangle with the letter n inside means the expansion of the wave function for the bound electron state n in terms of free electron wave functions

For the diagonal matrix element $n = a$ (which corresponds to the lowest order SE contribution to the Lamb shift) this convergence was observed quite well in several calculations [14,15,16]. In [14] the numerical approach called "space discretization" (the solution of the radial Dirac equation on the grid) was employed. The comparision with the most accurate first-order bound-electron self energy calculations by Mohr [16] where the numerical treatment was based on the use of the radial Green function for the bound-state Dirac equation indicates that taking about 30 partial waves into account is sufficient to reach an accuracy better than 0.1% for high Z values. The convergence with the number of partial waves l corresponding to the law l^{-3} was also observed [17]. Unfortunately, the PWE approach is unapplicable for lower Z values since it loses its accuracy due to the cancellations that occur between different terms.

This PWE renormalization method was also called "noncovariant" contrary to the "covariant" approach described above where the covariant procedure in 4-dimensional momentum space was used to separate out and cancel the divergent terms. In principle, the noncovariant procedure should not lead to any differences provided that both "bound"-term and counterterm are described in the same way. Such a difference may arise only if the counterterm, unlike the "bound"-term is written in covariant form [12].

The difficulty with low Z values can be avoided in another version of the noncovariant renormalization method, developed in [18,19]. Within this approach an explicit expression for the matrix element $\langle a|\gamma_0\hat{\Sigma}_{\rm bou}(E_a)|n\rangle$ is used:

$$\langle a|\gamma_0\hat{\Sigma}_{\rm bou}(E_a)|n\rangle = \frac{\alpha}{2\pi i}\sum_{n'}\langle an'|\frac{\gamma_\mu\gamma^\mu}{r_{12}}I(r_{12}\,\beta_{n'a})|n'n\rangle\ , \tag{14}$$

where the Dirac matrices γ_μ and γ^μ correspond to different variables $|n'(1)n(2)\rangle$, $\beta_{n'a} = E_{n'} - E_a$, $r_{12} = |\boldsymbol{r_1} - \boldsymbol{r_2}|$ and $I(r_{12}\,\beta_{n'a})$ is defined as

$$I(r_{12}\,\beta_{n'a}) = \int\limits_{-\infty}^{\infty} d\omega \frac{e^{-i|\omega|r_{12}}}{E_{n'}(1-i0) - E_a + \omega}\ . \tag{15}$$

Using the multiple commutator approach [20] where $I(r_{12}\,\beta_{n'a})$ is expanded in terms of $r_{12}\,\beta_{n'a}$ and the powers of $r_{12}\,\beta_{n'a}$ are replaced by the multiple

commutators with the Dirac one-electron Hamiltonian, one can show that most of the commutators are canceled between "bound" and "free" terms in Eq. (12). The remaining "bound" expression is given by [18,19]

$$\langle a|\gamma_0\hat{\Sigma}_{\rm bou}(E_a)|n\rangle = \frac{\alpha}{\pi}\sum_{n'}\langle an|\frac{\gamma_\mu\gamma^\mu}{r_{12}}\Big(\ln|E_a-E_{a'}|\sin((E_a-E_{a'})r_{12}) + \frac{\pi}{2}\mathrm{sgn}(E_{n'})\cos((E_a-E_{a'})r_{12})\Big)|n'n\rangle\ . \tag{16}$$

In the "free" electron counterterm the bound state wave functions $|a\rangle$ and $|n\rangle$ are expanded in terms of free electron states. Unlike [14,15,17] where the plane-wave-type functions were used for this purpose, the spherical-wave-type functions were employed in [18]. The summation over n' in Eq. (16) is replaced by the integration over the continuous quantum number p, defining the energy of the free electron $E_p = \pm\sqrt{p^2+m^2}$, and the summation over the standard angular quantum numbers j, l, m. An important difference between the standard numerical PWE procedure [14,15,16,17] and the version used in [18] is that in [18] only terms diagonal in p, j, l, m are retained in the counterterm after expansion of the bound states $\langle a|$ and $|n\rangle$. The motivation is that the interaction with the vacuum cannot change the exact free-electron quantum numbers.

This PWE was used in [18] to obtain the numerical results. For the numerical implementation the B-spline approximation [21] was chosen that represents actually the refined version of the "space discretization" approach. In Table 1 the convergence of the PWE approach with the multicommutator expansion is presented for the lowest-order SE correction for the ground state of hydrogen-like ions with $Z = 10$. The minimal set of parameters for the numerical spline calcuations was chosen to be: the number of grid points $N = 20$, the number of splines $k = 9$. This minimal set allowed to keep a controlled inaccuracy below 10%. What is most important for the further generalization of the PWE approach to the second-order SESE calculation is that with $l_{\rm max} = 3$ the inaccuracy is already below 10% (see Table 1). The same picture holds with even higher accuracy for larger Z values. The "direct" renormalization approach is not necessarily connected with the PWE. In [19] this approach in the form of the multicommutator expansion (Eq. (16)) was employed in combination with the Taylor expansion in powers of $(E_a - E_{n'})r_{12}$. The numerical procedure with the use of B-splines and 3 terms of Taylor series yielded an accuracy comparable with the PWE-expansion with $l_{\rm max} = 3$.

We now return to the loop-after-loop SESE calculations in [11]. The first two terms of the potential expansion Eq. (2), ZP and OP terms were evaluated in momentum space. For this purpose the Fourier transform was performed for the bound state wave functions $|n\rangle$ in coordinate space. The latter were evaluated by the "space discretization" method. The MP term was calculated entirely in coordinate space.

An investigation devoted to the evaluation of SESE a) irreducible contribution was accomplished by S. Mallampalli and J. Sapirstein [22]. Using the same covariant renormalization approach with the potential expansion and employing

Table 1. Convergence of PWE approach with the multicommutator expansion (Eq. 16) for the lowest-order SE correction for the ground-state of H-like ion with $Z = 10$. The accumulated sums $\triangle E^{(l)}_{1s} = \sum_{l'=0}^{l} \langle 1s|\gamma_0 \hat{\Sigma}^{(1)\mathrm{ren}(l')}_{\mathrm{bou}}|1s\rangle$ are given for 7 partial waves. The extrapolation formula was $\triangle E^{(1)}_{1s\,\mathrm{ex}} = \frac{1}{2}(\triangle E_{1s}(l_{\max}) + \triangle E_{1s}(l_{\max}+1))$ for different $l_{\max}$. All the values in eV

l	$\triangle E^{(l)}_{1s}$	$\triangle E^{(1)}_{1s,\mathrm{ex}}$	$\triangle E^{(1)}_{1s}$ [16]	Deviation
0	0.1269		0.1566	
1	0.1769			
2	0.1615	0.1692		
3	0.1715			8.0%
4	0.1659			
5	0.1702			
6	0.1672	0.1688		7.8%

a more refined numerical B-spline approach the authors were able to continue their results to the lower Z values up to $Z = 1$. For large Z their results coincided with [11].

In the low Z limit the results of [22] for the SESE a) irreducible contribution disagree with the results of the perturbation theory in $Z\alpha$ [23,24]. Actually the disagreement concerns the coefficient $-8/27$ of the $\ln^3(Z\alpha)^{-2}$ term found analytically by Karshenboim [25]. This disagreement became a subject of several controversal statements made in a series of subsequent papers [26,27,28]. The Mallampalli and Sapirstein result [22] would imply that PT in αZ is in principle inapplicable even for $Z = 1$.

The work [26] was devoted to the application of the PWE renormalization approach to the evaluation of the SESE a) irreducible contribution. In this work the multicommutator expansion version of the PWE [18] and the numerical B-spline approach was used. The results disagree strongly with Mallampalli and Sapirstein calculations for low and intermediate Z values but agree with [23,24,25].

In the publication by Yerokhin [27] the results of Mallampalli and Sapirstein [22] were confirmed. The analysis performed in [27] for the low-Z region, confirmed, that the graph shown in Fig. 6a) provides the Karshenboim $\ln^3(\alpha Z)^{-2}$ term. Moreover, it was found that the cubic logarithmic term arises also from the graph Fig. 6b). The latter was never observed by an analytic analysis in [25,28]. Yerokhin's analysis was based on the numerical fit. Recently a new analytic analysis in terms of the renormalization group [29] has been presented that contradicts to Yerokhin's conclusions.

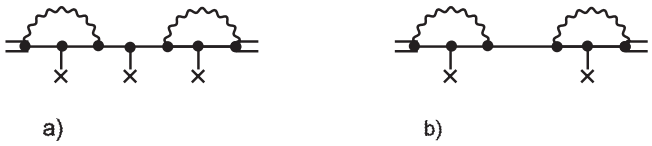

Fig. 6. Feynman graphs responsible for the $\ln^3(2Z)^{-2}$ contribution to the irreducible SESE a) graph in the low Z region. The graph a) yields the Karshenboim term, the graph b) corresponds to the additional Yerokhin term

Summarizing, we can say that while the discrepancy between the different calculations of the SESE a) irreducible contribution for low and intermediate Z values is still to be resolved, there are no reasons to doubt the applicability of the PWE method for high Z regions where all the methods give stable coincident results.

3 Other SESE contributions

In this section we will calculate the reducible contributions to the graph Fig. 1 a) and the total contributions to the graphs Figs. 1b),1c). The general renormalization scheme for these graphs was presented in [30]. This scheme exploits the potential expansion for separating out the divergent terms and is suitable for the application of the PWE approach. Later these results were rederived in [31] by a different method.

The renormalized expression for the two-photon self energy $\triangle E_a^{(z)\mathrm{ren}}$ (without the irreducible SESE a) term) for the bound-electron state $|a\rangle$ reads [30]:

$$\triangle E_a^{(2)\mathrm{ren}} = \triangle E_a^{(\mathrm{red})\mathrm{ren}} + \triangle E_a^{(\mathrm{in})\mathrm{ren}} + \triangle E_a^{(\mathrm{cr})\mathrm{ren}} + \triangle E_a^{(\mathrm{ac})\mathrm{ren}} \,, \tag{17}$$

$$\triangle E_a^{(\mathrm{red})\mathrm{ren}} = \langle a|\gamma_0 \hat{\Sigma}_{\mathrm{bou}}^{(1)\mathrm{ren}}(E_a)|a\rangle \left[\frac{\partial}{\partial E}\langle a|\gamma_0 \hat{\Sigma}_{\mathrm{bou}}^{(1)\mathrm{ren}}(E)|a\rangle\right]_{E=E_a} \,, \tag{18}$$

$$\triangle E_a^{(\mathrm{in})\mathrm{ren}} = \triangle E_a^{(\mathrm{in})} - \delta m^{(\mathrm{in})}\langle a|\gamma_0|a\rangle \,, \tag{19}$$

$$\triangle E_a^{(\mathrm{cr})\mathrm{ren}} = \triangle E_a^{(\mathrm{cr})} - \delta m^{(\mathrm{cr})}\langle a|\gamma_0|a\rangle \,, \tag{20}$$

$$\triangle E_a^{(\mathrm{ac})\mathrm{ren}} = -\delta m^{(1)}\left[\langle a|\gamma_0 \hat{\tilde{\Sigma}}_{\mathrm{bou}}^{(1)}(E_a)|a\rangle - \delta\tilde{m}^{(1)}\langle a|\gamma_0|a\rangle\right] . \tag{21}$$

As indicated by subscripts the various terms here denote the reducible loop-after-loop (red), the loop-inside-loop (in), the crossed-loops (cr) contributions and an additional counter term (ac) to the SESE b) graph, respectively. The subscript ren always signifies the renormalized expression, though the expressions $\triangle E_a^{(\mathrm{red})\mathrm{ren}}$, $E_a^{(\mathrm{in})\mathrm{ren}}$, $E_a^{(\mathrm{cr})\mathrm{ren}}$ and $E_a^{(\mathrm{ac})\mathrm{ren}}$ are individually still ultraviolet divergent. This happens since some of the counterterms cancel each other in Eq. (17). Furthermore, all these expressions also contain infrared divergencies, that arise in the process of renormalization. However, all ultraviolet and infrared divergencies are going to vanish in the combination they appear in Eq. (17) [30].

The terms $\triangle E_a^{(\mathrm{in})}$, $\triangle E_a^{(\mathrm{cr})}$ represent the unrenormalized bound-electron expressions and $\delta m^{(\mathrm{in})}$, $\delta m^{(\mathrm{cr})}$ are the corresponding counterterms. The additional counterterm $\triangle E^{(\mathrm{ac})\mathrm{ren}}$ has been derived in [30] and later confirmed in [31]. It contains the first-order bound-electron self energy operator $\tilde{\hat{\Sigma}}_{\mathrm{bou}}$ with quadratic denominator (see an explicit expression) and the corresponding first-order counterterm $\delta\tilde{m}^{(1)}$.

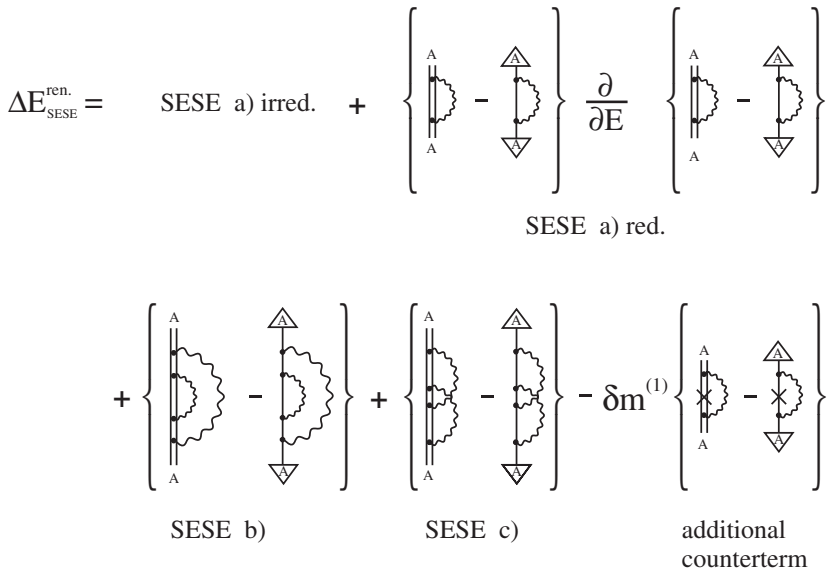

Fig. 7. The graphical represantation of the "direct" PWE renormalization approach. The double and ordinary solid lines with the cross denote the quadratic denominators in the bound and free electron propagators. The other notations are the same as in Figure 5. The graphs a)–c) correspond to Eqs. (18)–(20) and the additional counterterm correspond to Eq. (21), respectively

Eq. (17) is an analogy of the first-order diagonal ($n = a$) equation (11). In Fig. 7 an analogy of Fig. 5, i.e., the graphical representation of the PWE renormalization approach to $\triangle E_a^{(2)\mathrm{ren}}$ is depicted. Below we give the explicit expressions for all contributions from the graphs with double electron lines in Fig. 7, i.e., "bound" electron terms:

$$\left[\frac{\partial}{\partial E}\langle a|\gamma_0\hat{\Sigma}^{(1)}_{bou}(E)|a\rangle\right]_{E=E_a} = \frac{i\alpha}{2\pi}\sum_n \int_{-\infty}^{\infty} d\omega \frac{\langle an|\gamma_\mu\gamma^\mu \frac{\exp(i|\omega|r)}{r}|na\rangle}{(E_a-\tilde{E}_n-\omega)^2}\ , \quad (22)$$

$$\triangle E_a^{(\mathrm{in})} = -\frac{\alpha^2}{4\pi^2}\sum_{p,q,r}\int_{-\infty}^{\infty} d\omega \int_{-\infty}^{\infty} d\omega'$$

$$\times \frac{\langle ar|\gamma_\mu\gamma^\mu \frac{\exp(i|\omega|r)}{r}|pa\rangle\langle pq|\gamma_\mu\gamma^\mu \frac{\exp(i|\omega'|r)}{r}|qr\rangle}{(E_a-\tilde{E}_p-\omega)(E_a-\tilde{E}_q-\omega-\omega')(E_a-\tilde{E}_r-\omega)} , \quad (23)$$

$$\triangle E_a^{(\mathrm{cr})} = -\frac{\alpha^2}{4\pi^2}\sum_{p,q,r}\int_{-\infty}^{\infty} d\omega \int_{-\infty}^{\infty} d\omega' ,$$
$$\times \frac{\langle aq|\gamma_\mu\gamma^\mu \frac{\exp(i|\omega|r)}{r}|pr\rangle\langle pr|\gamma_\mu\gamma^\mu \frac{\exp(i|\omega'|r)}{r}|qa\rangle}{(E_a-\tilde{E}_p-\omega')(E_a-\tilde{E}_q-\omega-\omega')(E_a-\tilde{E}_r-\omega)} , \quad (24)$$

$$\langle a|\gamma_0\hat{\tilde{\Sigma}}^{(1)}_{\mathrm{bou}}(E_a)|a\rangle = \frac{i\alpha}{2\pi}\sum_{p,q}\int_{-\infty}^{\infty} d\omega \frac{\langle ap|\gamma_\mu\gamma^\mu \frac{\exp(i|\omega|r)}{r}|qa\rangle\langle q|\gamma_0|p\rangle}{(E_a-\tilde{E}_p-\omega)(E_a-\tilde{E}_a-\omega)} . \quad (25)$$

Here $r = r_{12}$ and $\tilde{E}_n = E_n(1-i0)$, so that the Feynman rules for the integration over ω variables are assumed. All sums run over the complete Dirac spectrum for the electron in the field of the nucleus. The expressions for the counterterms are:

$$\delta m^{(\mathrm{in})} = 4\pi i\alpha \int \frac{d^4k}{(2\pi)^4}\gamma_\mu \frac{1}{\not p-\not k-m}\hat{\Sigma}^{(1)}(\not p-\not k)\frac{1}{\not p-\not k-m}\gamma^\mu \frac{1}{k^2}|_{\not p=m} , \quad (26)$$

$$\delta m^{(\mathrm{cr})} = 4\pi i\alpha \int \frac{d^4k}{(2\pi)^4}\hat{\Lambda}^{(1)}_\mu(\not p,\not p-\not k)\frac{1}{\not p-\not k-m}\gamma^\mu \frac{1}{k^2}|_{\not p=m} , \quad (27)$$

$$\tilde{\delta} m^{(\mathrm{in})} = 4\pi i\alpha \int \frac{d^4k}{(2\pi)^4}\gamma_\mu \frac{1}{(\not p-\not k-m)^2}\gamma^\mu \frac{1}{k^2}|_{\not p=m} . \quad (28)$$

In this paper we adopt the PWE renormalization scheme. Accordingly, all "bound" terms in Eqs. (18)–(21) appear as double sums over partial waves. These double sums arise from the product of two matrix elements containing $\exp(i|\omega|r)$. Each individual partial wave contribution is finite and only the sum over partial waves diverges. In our calculation this divergency is removed by term-by-term subtraction of the corresponding counterterms. The PWE for the sum of all terms in Eq. (17) thus ensures a correct cancellation.

Within the PWE approach, using the expansion of the bound state $|a\rangle$ in terms of the free-electron spherical wave functions, we write the counterterms in the form:

$$\delta m^{(1)} = \frac{i\alpha}{2\pi}\int_0^\infty dp\, \langle a|pjlm\rangle^*\langle pjlm|a\rangle \int_0^\infty dq \sum_{j',l',m'}\int_{-\infty}^{\infty} d\omega$$
$$\times \frac{\langle pjlm, qj'l'm'|\gamma_\mu\gamma^\mu \frac{\exp(i|\omega|r)}{r}|qj'l'm', pjlm\rangle}{(E_p-\tilde{E}_q-\omega)} , \quad (29)$$

$$\delta m^{(\mathrm{in})} = \frac{-\alpha^2}{4\pi^2}\int_0^\infty dp\, \langle a|pjlm\rangle^*\langle pjlm|a\rangle$$

$$\times \int_0^\infty ds \sum_{j',l',m'} \int_0^\infty dq \sum_{j'',l'',m''} \int_0^\infty dt \sum_{j'',l'',m''} \int_{-\infty}^{\infty} d\omega \int_{-\infty}^{\infty} d\omega'$$
$$\times \frac{\langle pjlm, tj'''l'''m''' | \gamma_\mu \gamma^\mu \frac{\exp(i|\omega|r)}{r} | sj'l'm', pjlm \rangle}{(E_p - \tilde{E}_q - \omega - \omega')}$$
$$\times \frac{\langle pjlm, qj''l''m'' | \gamma_\mu \gamma^\mu \frac{\exp(i|\omega|r)}{r} | qj''l''m'', tj'''l'''m''' \rangle}{(E_p - \tilde{E}_s - \omega)(E_p - \tilde{E}_t - \omega)} , \qquad (30)$$

$$\delta m^{(\mathrm{cr})} = \frac{-\alpha^2}{4\pi^2} \int_0^\infty dp \, \langle a|pjlm\rangle^* \langle pjlm|a\rangle$$
$$\times \int_0^\infty ds \sum_{j',l',m'} \int_0^\infty dq \sum_{j'',l'',m''} \int_0^\infty dt \sum_{j'',l'',m''} \int_{-\infty}^{\infty} d\omega \int_{-\infty}^{\infty} d\omega'$$
$$\times \frac{\langle pjlm, qj''l''m'' | \gamma_\mu \gamma^\mu \frac{\exp(i|\omega|r)}{r} | sj'l'm', tj'''l'''m''' \rangle}{(E_p - \tilde{E}_q - \omega - \omega')}$$
$$\times \frac{\langle s'j'l'm', tj'''l'''m''' | \gamma_\mu \gamma^\mu \frac{\exp(i|\omega|r)}{r} | qj'l'm', pjlm \rangle}{(E_p - \tilde{E}_s - \omega')(E_p - \tilde{E}_t - \omega)} , \qquad (31)$$

$$\delta \tilde{m}^{(1)} = \frac{i\alpha}{2\pi} \int_0^\infty dp \, \langle a|pjlm\rangle^* \langle pjlm|a\rangle \int_0^\infty ds \sum_{j',l',m'} \int_0^\infty dq \sum_{j'',l'',m''} \int_{-\infty}^{\infty} d\omega$$
$$\times \frac{\langle pjlm, sj'l'm' | \gamma_\mu \gamma^\mu \frac{\exp(i|\omega|r)}{r} | qj''l''m'', pjlm \rangle}{(E_p - E_s - \omega)(E_p - \tilde{E}_q - \omega)}$$
$$\times \langle qj''l''m'' | \gamma_0 | sj'l'm' \rangle . \qquad (32)$$

Here $|pjlm\rangle$ denotes the spherical-wave free-electron function with the usual notations for Dirac angular quantum numbers. The numbers jlm are fixed by the overlap with the bound-electron wave function $|a\rangle \equiv |njlm\rangle$ where n is the principal quantum number. Integration over p is interpreted as integration over energies $E_p = \pm\sqrt{p^2 + m^2}$.

For the evaluation of the sums over the Dirac spectrum the B-spline approximation has been employed. The number of grid points N and the order of splines k have been chosen to be $N = 23$ and $k = 4$, respectively. This corresponds to 50 different radial Dirac states which are taken into account for a given Dirac angular-momentum quantum number.

For the integration over ω, ω' a following transformation was made in Eq. (23)

$$
\begin{aligned}
I^{(\mathrm{in})} &\equiv \int_{-\infty}^{\infty} d\omega \int_{-\infty}^{\infty} d\omega' \frac{\exp(i|\omega|r)\exp(i|\omega'|r')}{(\tilde{\triangle}_{ap}-\omega)(\tilde{\triangle}_{aq}-\omega-\omega')(\tilde{\triangle}_{ar}-\omega)} \qquad (33)\\
&= \int_{0}^{\infty} d\omega \int_{0}^{\infty} d\omega' \, \sin(\omega r)\, \sin(\omega' r)\\
&\times \frac{1}{(\triangle_{pa}+\omega\mathrm{sign}(E_p))(\triangle_{qa}+(\omega+\omega')\mathrm{sign}(E_q))(\triangle_{ra}+E_r\mathrm{sign}(\omega))}\\
&\times \left(1+\frac{1}{\triangle_{rp}}\left[\frac{\omega(\mathrm{sign}(E_p)-\mathrm{sign}(E_q))(\triangle_{ra}+\omega\mathrm{sign}(E_r))}{\triangle_{pq}-\omega'\mathrm{sign}(E_q)} \right.\right.\\
&\left.\left. -\frac{\omega(\mathrm{sign}(E_r)-\mathrm{sign}(E_q))(\triangle_{pa}+\omega\mathrm{sign}(E_p))}{\triangle_{rq}-\omega'\mathrm{sign}(E_q)} \right] \right)\\
&\equiv \int_{0}^{\infty} d\omega \int_{0}^{\infty} d\omega' \; F^{(\mathrm{in})}(\omega,\omega')(1+S^{(\mathrm{in})}(\omega,\omega')) \, ,
\end{aligned}
$$

where $\triangle_{pq} = E_p - E_q$ etc.

The advantage of Eq. (33) is the possibility of neglecting the term containing $S^{(\mathrm{in})}(\omega,\omega')$. This neglect is due to the presence of large denominators of the type $E_p - E_q - \omega'\mathrm{sign}(E_q)$. Remembering that this denominator is combined with the numerator $\mathrm{sign}(E_p) - \mathrm{sign}(E_q)$ we obtain for $E_p > 0, E_q < 0$ the behaviour $E_p - E_q - \omega'\mathrm{sign}(E_q) \geq 2m$ and the behaviour $E_p - E_q - \omega'\mathrm{sign}(E_q) \leq -2\ m$ for the opposite case. For large $\omega, \omega' \geq 10\ m$ the terms with $S^{(\mathrm{in})}(\omega,\omega')$ begin to oscillate strongly what is evidently connected with the numerical instability and has no physical background since in principle the integral $I^{(\mathrm{in})}$ converges. We therefore cut off the oscillating part at $10\ m$. The remainer of $S^{(\mathrm{in})}(\omega,\omega')$ contribution is then negligible compared to 1 in Eq. (33). The same situation arises also for the integral $I^{(\mathrm{cr})}$.

For the terms, containing only $F^{(\mathrm{in})}(\omega,\omega')$, $F^{(\mathrm{cr})}(\omega,\omega')$ functions the integration is extended up to $465\ m$.

Within our approach the major source for inaccuracies is the different treatment of the bound-state terms and free-electron counterterms, since the B-spline representation of the latter terms generates severe numerical difficulties. Therefore, we prefered to add and subtract zero-potential terms of the potential expansion Fig. 4 to each individual expression in Eq. (17). Zero-potential terms differ from the bound-electron terms by the substitution of the bound-state propagators by the free-electron ones but keeping the bound-state energy E_a in the energy denominators. Differences between each of the bound-electron terms and corresponding zero-potential in Eq. (17) can be evaluated equally well within the B-spline approach. The evaluation of the remaining differences

between zero-potential terms and counterterms can be accomplished semianalytically. A similar procedure has been already utilized earlier in the calculation of the first-order electron self energy [17,18]. This diminishes the inaccuracy in the numerical calculations which in our case still remains rather high: about 40%. This inaccuracy was determined by the unstability of the results with the change of the number of grid points from $N = 23$ to $N = 46$.

The individual terms $\triangle E_{1s}^{l_1,l_2}$ of the double partial-wave expansion

$$\triangle E_{1s}^{(2)\mathrm{ren}} = \sum_{l_1,l_2} \triangle E_{1s}^{l_1,l_2} \tag{34}$$

for uranium ($Z = 92$) and lead ($Z = 82$) H-like ions are listed in the Tables 2,3.

Table 2. Partial-wave contributions $\triangle E_{1s}^{(l_1,l_2)}$ to $\triangle E_{1s}^{(2)\mathrm{ren}}$ for the H-like U ion (in eV)

	$l_2 = 0$	$l_2 = 1$	$l_2 = 2$	$l_2 = 3$
$l_1 = 0$	0.699	0.384	0.106	−0.059
$l_1 = 1$	0.384	−0.188	0.563	
$l_1 = 2$	−0.427	−0.376		
$l_1 = 3$	0.501			

Table 3. Partial-wave contributions $\triangle E_{1s}^{(l_1,l_2)}$ to $\triangle E_{1s}^{(2)\mathrm{ren}}$ for the H-like Pb ion (in eV)

	$l_2 = 0$	$l_2 = 1$	$l_2 = 2$	$l_2 = 3$
$l_1 = 0$	0.439	0.158	0.051	−0.04
$l_1 = 1$	0.186	−0.092	0.228	
$l_1 = 2$	−0.135	−0.124		
$l_1 = 3$	0.172			

The inaccuracy of our calculations is determined by the unstability of numerical results with the change of the number of grid points from $N = 23$ to $N = 46$. This unstability can be as large as 38% (SESE b), $l_1 = 2$, $l_2 = 0$, $Z = 82$). However, we can consider these errors as statistical, not systematical. It follows from the Tables 2,3 where nearly one half of the values have the opposite signs. Then in the sum Eq. (38) this inaccuracy should decline as $1/\sqrt{n}$, where n is the number of terms, in our case $n = 10$, so that we estimate the final inaccuracy as 12%. The other argument is that for same reason the final inaccuracy should not exceed too much the absolute inaccuracy for the one term

Table 4. Lamb shift contribution for the ground state of $^{238}U^{91+}$ ion (in eV). Here R_0 denotes the nuclear radius, M is nuclear mass and a_0 is the Bohr radius. The finite nuclear-size correction is calculated for a Fermi distribution with $\langle r^2\rangle^{1/2} = 5.860\pm0.002$ fm. The corrections VPVP (f) and S(VP)E are known only in Uehling approximation. The inaccuracies assigned to these rather small corrections are estimated as the average of the inaccuracies of the Uehling approximation deduced from exact results for the corrections VPVP (e) and SEVP (g),(h),(i)

Correction	Order of magnitude and scaling with Z	Numerical value	Reference
Binding energy	$m(\alpha Z)^2$	-132279.66	
Finite nuclear size	$m(RZ/a_0)^2$	198.82 ± 0.10	[3]
Electron self energy	$m\alpha(\alpha Z)^4$	355.05	[3]
Vacuum polarization	$m\alpha(\alpha Z)^4$	-88.60	[3]
Total first-order QED	$m\alpha(\alpha Z)^4$	266.45	
SESE (a) (irred)	$m\alpha^2(\alpha Z)^5$	-0.97	[11,22,26]
SESE (a) (red), (b),(c)	$m\alpha^2(\alpha Z)^4$	1.28 ± 0.15	This work
VPVP (d)	$m\alpha^2(\alpha Z)^5$	-0.22	[7,8,35]
VPVP (e)	$m\alpha^2(\alpha Z)^4$	-0.153	[4,5,6]
VPVP (f) (Uehling)	$m\alpha^2(\alpha Z)^4$	-0.60 ± 0.01	[4,5]
SEVP (g),(h),(i)	$m\alpha^2(\alpha Z)^5$	1.12	[8,9]
S(VP)E (Uehling)	$m\alpha^2(\alpha Z)^5$	0.13	[8,10]
Total second-order QED		0.59 ± 0.16	
Relativistic recoil	$m(m/M)(\alpha Z)^2$	0.16	[36,37]
Nuclear polarization		-0.2 ± 0.1	[38]
Lamb shift (theory)		465.82 ± 0.26	
Lamb shift (experiment)		469 ± 13	[1]

of the double PWE. In the example given above this absolute inaccuracy is 0.09 eV. The final value $\triangle E_{1s}^{(2)\mathrm{ren}}$ was obtained by an extrapolation from the numbers given in Tables 2,3. Accordingly, we evaluated the accumulated sums

$$S_l = \sum_{l_1,l_2}^{l_1+l_2=l} \triangle E_{1s}^{(l_1,l_2)} \tag{35}$$

for $l = 0, 1, 2$ and 3. Corresponding values in eV for U and Pb are

$$\mathrm{U}: \quad S_0 = 0.70, \quad S_1 = 1.47, \quad S_2 = 0.96, \quad S_3 = 1.59\,, \tag{36}$$

$$\mathrm{Pb}: \quad S_0 = 0.439, \; S_1 = 0.783, \; S_2 = 0.607, \; S_3 = 0.843\,. \tag{37}$$

Table 5. Lamb shift contribution for the ground state of $^{208}Pb^{81+}$ ion (in eV). The notations are the same as in Table 4. The finite nuclear size correction is calculated for a Fermi distribution with $\langle r^2\rangle^{1/2} = 5.505 \pm 0.001$ fm. The SESE (a) (irred) correction is obtained by an interpolation from the known values for $Z = 70, 80, 92$. The inaccuracy of the Uehling approximation for VPVP (f) and S(VP)E corrections is neglected. The zero value presented for the nuclear polarization is due to the cancellation of the usual nuclear polarization [35] with the mixed nuclear polarization (NP)-vacuum polarization correction [36]. The latter effect arises when the nucleus interacts with a virtual electron-positron pair. For lead, due to the collective monopole vibrations, specific for this nucleus, mixed NP-VP effect becomes rather large. Therefore, the nuclear polarization effects which otherwise limit very precise Lamb shift predictions are almost completely negligible for ^{208}Pb, making this ion especially suitable for the most precise theoretical predictions

Correction	Order of magnitude and scaling with Z	Numerical value	Reference
Binding energy	$m(\alpha Z)^2$	-101581.37	
Finite nuclear size	$m(RZ/a_0)^2$	67.25	[3]
Electron self energy	$m\alpha(\alpha Z)^4$	226.33	[3]
Vacuum polarization	$m\alpha(\alpha Z)^4$	-48.41	[3]
Total first-order QED	$m\alpha(\alpha Z)^4$	177.92	
SESE (a) (irred)	$m\alpha^2(\alpha Z)^5$	-0.51	[11]
SESE (a) (red), (b),(c)	$m\alpha^2(\alpha Z)^4$	0.73 ± 0.09	This work
VPVP (d)	$m\alpha^2(\alpha Z)^5$	-0.09	[7,8,35]
VPVP (e)	$m\alpha^2(\alpha Z)^4$	-0.07	[4,5,6]
VPVP (f) (Uehling)	$m\alpha^2(\alpha Z)^4$	-0.34	[4,5]
SEVP (g),(h),(i)	$m\alpha^2(\alpha Z)^5$	0.53	[8,9]
S(VP)E (Uehling)	$m\alpha^2(\alpha Z)^5$	0.07	[8,10]
Total second-order QED		0.32 ± 0.09	
Relativistic recoil	$m(m/M)(\alpha Z)^2$	0.10	[36,37]
Nuclear polarization		0.00	[38,39]
Lamb shift (theory)		245.59 ± 0.09	
Lamb shift (experiment)		290 ± 75	[40]

The extrapolation formula was the same as for the the first order (see Table 1). The results are

$$\begin{aligned} \triangle E_{1s}^{(2)\mathrm{ren}}(Z=92) &= 1.28 \pm 0.15 \text{ eV} , \\ \triangle E_{1s}^{(2)\mathrm{ren}}(Z=82) &= 0.73 \pm 0.09 \text{ eV} . \end{aligned} \tag{38}$$

We should stress that one should not require the convergence of $\triangle E_a^{(2)\mathrm{ren}}$ in both directions along $l_1$or l_2 in the two-dimensional space l_1, l_2. This kind of convergence would exist only in the case of the weak coupling between the two partial wave expansions in $\triangle E_a^{(2)\mathrm{ren}}$: e.g. when the two expansions are fully independent and factorize. The numbers in Tables 2,3 indicate that in our case the coupling is strong. The limit of the number of partial waves was set by the extremely large computer time required. The calculations were performed at the computer center of the Technical University of Dresden on the CRAY-T3E supercomputer with 32 parallel processors. The inclusion of 4 partial waves $l_1, l_2 = 0, 1, 2, 3$ in both PWE with the limitation $l_{\max} \leq 3$, $l = l_1 + l_2$ required more than 20 thousend single-processor CPU hours for each ion (U,Pb).

In Tables 4,5 we summarize all known corrections to the ground-state energy of hydrogen-like U and Pb ions including the complete set of the SESE corrections obtained in the present paper. The inaccuracy assigned to our results for SESE a) (red) + SESE b), c) corrections remains the main source of the total error in the theoretical Lamb shift prediction. We expect that the inaccuracy can be essentially diminished within the framework of the method described above.

Acknowledgements

The authors are indebted to Prof. Dr. W. Nagel and Dr. S. Seidel from the computer center of the TU Dresden for their help in optimizing the computer codes. They also wish to thank Dr. U. Jentschura for useful comments. I.G., L.L. and A.N. are gratefull to the Technische Universität Dresden and the Max-Planck-Institut für Physik komplexer Systeme (MPI) for the hospitality. They also acknowledge financial support from MPI, DFG and RFBR (Grant No. 99-02-18526). G.S., G.P. and S.Z. acknowledge financial support from BMBF, DFG and GSI.

References

1. T. Stöhlker *et al.*: The 1s Lamb Shift in Hydrogen-like Uranium Measured on Cooled, Decelerated Ion Beams, submitted to Phys. Rev. Lett.
2. Th. Beier, P.J. Mohr, H. Persson, G. Plunien, M. Greiner and G. Soff: Phys. Lett. **A 236**, 329 (1997)
3. P.J. Mohr, G. Plunien and G. Soff: Phys. Rep. **293**, 227 (1998)
4. Th. Beier and G. Soff: Z. Phys. **D 8**, 129 (1988)
5. S.M. Schneider, W. Greiner and G. Soff: J. Phys. **B 26**, L529 (1993).
6. G. Plunien, Th. Beier, G. Soff and H. Persson, Eur. Phys. J. **D 1**, 177 (1998)

7. H. Persson, I. Lindgren, S. Salomonson and P. Sunnergren: Phys. Rev. A **48**, 2772 (1993)
8. H. Persson, I. Lingren, L. N. Labzowsky, G. Plunien, Th. Beier and G. Soff: Phys. Rev. **A 54**, 2805 (1996)
9. I. Lindgren, H. Persson, S. Salomonson, V. Karasiev, L.N. Labzowsky, A.O. Mitrushenkov and M. Tokman: J. Phys. **B 26**, L503 (1993)
10. S. Mallampalli and J. Sapirstein: Phys. Rev. **A54**, 2714 (1996)
11. A.O. Mitrushenkov, L.N. Labzowsky, I. Lindgren, H. Persson and S. Salomonson: Phys. Lett. **A200**, 51 (1995)
12. G.E. Brown, J.S. Langer and G.W. Schayer: Proc. R. Soc. London **251**, 92 (1959)
13. S.A. Blundell and N.J. Snyderman: Phys. Rev. **A44**, R1427 (1991)
14. H. Persson, I. Lindgren and S. Salomonson: Phys. Scr. **T46**, 125 (1993); I. Lindgren and S. Salomonson and A. Ynnerman: Phys. Rev. **A 47**, R4555 (1993)
15. H.M. Quiney and I.P. Grant: Phys. Scr. **T 46**, 132 (1993); J. Phys. **B 27**, L299 (1994)
16. P.J. Mohr: Ann. Phys. (N.Y.) **88**, 26 (1974); Phys. Rev. **A 46**, 4421 (1992).
17. H. Persson: Ph.D. Thesis, Göteborg University, 1993.
18. L.N. Labzowsky, I.A. Goidenko and A.V. Nefiodov: J. Phys. **B 31**, L477 (1998)
19. Yu. Yu. Dmitriev, T.A. Fedorova and D.M. Bogdanov: Phys. Lett. **A 241**, 84 (1998)
20. L.N. Labzowsky and I.A. Goidenko: J. Phys. **B 30**, 177 (1997); I.A. Goidenko and L.N. Labzowsky: Zh. Eksp. Teor. Fiz. **112**, 1197 (1997) [Sov. Phys. JETP **85**, 650 (1997)].
21. W.R. Johnson, S.A. Blundell and J. Sapirstein: Phys. Rev. **A 37**, 307 (1988)
22. S. Mallampalli and J. Sapirstein: Phys. Rev. Lett. **80**, 5297 (1998)
23. K. Pachucki: Phys. Rev. Lett. **72**, 3154 (1994)
24. M.I. Eides and V.A. Shelyuto: Zh. Eksp. Teor. Fiz. **61**, 465 (1995) [JETP Lett. **61**, 478 (1995)]; Phys. Rev. **A 52**, 954 (1995)
25. S.G. Karshenboim: Zh. Eksp. Teor. Fiz. **103**, 105 (1993) [Sov. Phys. JETP **76**, 541 (1993)]
26. I.A. Goidenko, L.N. Labzowsky, A.V. Nefiodov, G. Plunien and G. Soff: Phys. Rev. Lett. **83**, 2312 (1999)
27. V.A. Yerokhin: Phys. Rev. **62**, 012508 (2000)
28. M.A. Eides, H. Grotch and V.A. Shelyuto: Theory of Light Hydrogen-like Atoms, hep-ph/0002158.
29. A.V. Manohar and I.W. Stewart: hep-ph/0004018.
30. L.N. Labzowsky and A.O. Mitrushenkov: Phys. Lett. **A 198**, 333 (1995); Phys. Rev. **A 53**, 3029 (1996).
31. I. Lindgren, H. Persson, S. Salomonson and P. Sunnergren: Phys. Rev. **A 58**, 1001 (1998)
32. Th. Beier, G. Plunien, M. Greiner and G. Soff: J. Phys. **B 30**, 2761 (1997)
33. A.N. Artemyev, V.M. Shabaev and V.A. Yerokhin: Phys. Rev. **A 52**, 1884 (1995)
34. V.M. Shabaev, A.N. Artemyev, Th. Beier, G. Plunien, V.A. Yerokhin and G. Soff: Phys. Rev. **A 57**, 4235 (1998)
35. G. Plunien, B. Müller, W. Greiner and G. Soff: Phys. Rev. **A 43**, 5853 (1991); G. Plunien and G. Soff: Phys. Rev. **A 53**, 4614 (1996); A.V. Nefiodov, L.N. Labzowsky, G. Plunien and G. Soff: Phys. Lett. **A 222**, 227 (1996)
36. L.N. Labzowsky, A.V. Nefiodov, G. Plunien, Th. Beier and G. Soff: J. Phys. **B 29**, 3841 (1996)
37. P.H. Mokler, Th. Stöhlker, C. Kozhuharov, R. Moshammer, P. Rymuza, Z. Stachura and A. Warczak: J. Phys. **28**, 617 (1995)